Chemical Communications

SUPPORTING INFORMATION

Tuning the Lewis Acidity of Difluorido Gold(III) Complexes: Synthesis of [$AuClF_2$(SIMes)] and [$AuF_2(OTeF_5)$(SIMes)]

Mathias A. Ellwanger, Clara von Randow, Simon Steinhauer, Yunfei Zhou, Anja Wiesner,
Helmut Beckers, Thomas Braun and Sebastian Riedel*

Experimental section 2
- CAUTION Strong Oxidizers! 2
- Materials and Chemicals 2
- Synthesis of [AuF_3(SIMes)], 1 2
- Comment on the Synthesis and Purification of [AuF_3(SIMes)], 1 3
- Synthesis of [$AuClF_2$(SIMes)], 2 4
- Crystal growth of [$AuClF_2$(SIMes)], 2 4
- Synthesis of [$AuF_2(OTeF_5)$(SIMes)], 3 4
- Crystal growth of [$AuF_2(OTeF_5)$(SIMes)], 3 5
- Synthesis of $Me_3Si(OTeF_5)$ 5
- Crystal growth of $Me_3Si(OTeF_5)$ 5

X-ray crystallography 6
- Structure of [$AuClF_2$(SIMes)], 2 7
- Structure of [$AuF_2(OTeF_5)$(SIMes)]$\cdot CH_2Cl_2$, 3a 7
- Structure of [$AuF_2(OTeF_5)$(SIMes)]$\cdot 0.4(C_6F_2H_4)\cdot 0.4(HOTeF_5)$, 3b 8

NMR spectroscopy 9
- Summary of NMR parameters 9
- Spectra of [AuF_3(SIMes)], 1 10
- Spectra of [$AuClF_2$(SIMes)], 2 10
- Spectra of [$AuF_2(OTeF_5)$(SIMes)], 3 11

Vibrational spectroscopy 12
- Overview 12
- Spectra of [AuF_3(SIMes)], 1 12
- Spectra of [$AuClF_2$(SIMes)], 2 13
- Spectra of [$AuF_2(OTeF_5)$(SIMes)], 3 13
- Spectra of $Me_3Si(OTeF_5)$ 14

Quantum-chemical calculations 15
- Comparison of SIMes affinity with FIA values 15

References 16

Experimental section

CAUTION Strong Oxidizers!

All materials must be handled under rigorously anhydrous conditions. Contact of AuF_3 with organic compounds can result in a violent reaction. All used fluoride containing materials decompose under formation of HF upon contact with small amounts of moisture. Immediate access to proper treatment procedures in case of contact with HF-containing solutions must be ensured.

Materials and Chemicals

The experiments were performed under rigorous exclusion of moisture and ambient air using standard Schlenk techniques. All solid materials were handled inside a glove box with an atmosphere of dry argon ($O_2 < 0.5$ ppm, $H_2O < 0.5$ ppm). Solvents were dried prior to use with CaH_2 as in case of CH_2Cl_2, CD_2Cl_2, $C_6F_2H_4$, n-pentane and Me_3SiCl. The compounds AuF_3 [1,2] and $HOTeF_5$ [3] were prepared by literature methods. 1,3-Bis-(2,4,6-trimethylphenyl)-2-imidazolidinyliden (SIMes) was prepared from 1,3-Bis(2,4,6-trimethylphenyl)-imidazolidinium chloride which was used as purchased and deprotonated as described in the literature.[4]

Raman spectra were recorded on a Bruker MultiRAM II equipped with a low-temperature Ge detector (1064 nm, 20-30 mW for all gold containing compounds and 125 mW for $Me_3Si(OTeF_5)$, resolution 4 cm^{-1}). IR spectra were either measured on a Bruker ALPHA FTIR spectrometer equipped with a diamond ATR attachment in a glove box filled with argon or on a Bruker Vector 22 with a gas cuvette equipped with silicon windows (0.5 mm). NMR spectra were recorded on a JEOL 400 MHz ECS or ECZ spectrometer. Chemical shifts are referenced to the standards $(CH_3)_4Si$ (^1H, ^{13}C and ^{29}Si) and $CFCl_3$ (^{19}F). Crystal data were collected on a Bruker D8 Venture CMOS area detector diffractometer with MoK_α radiation. Single crystal were picked at room temperature in case of $[AuF_3(SIMes)]$, $[AuF_2(OTeF_5)(SIMes)]$ and at –80 °C in case of $Me_3Si(OTeF_5)$ under nitrogen atmosphere and mounted on a 0.15 mm Mitegen micromount using perfluoroether oil. The structure was solved with the ShelXT[5] structure solution program using intrinsic phasing and refined with the ShelXL[6] refinement package using Least Squares minimizations by using OLEX2.[7] The CCDC 1850339, 1849407, 1850338, 1851138 contains the supplementary crystallographic data for this paper. These data can be obtained free of charge from the Cambridge Crystallographic Data Centre. For quantum chemical calculations the program package, functionals (B3LYP[8] with RI[9] and Grimme-D3[10]) and the basis sets (def2-TZVPP[11,12]) were used as implemented in TURBOMOLE.[13]

Synthesis of $[AuF_3(SIMes)]$, 1

In a typical experiment AuF_3 (20.5 mg, 81 µmol, fine powdered) and SIMes (24.4 mg, 80 µmol) were weighed into a Schlenk flask. Dichloromethane (5-6 ml) was condensed on top at –80 °C and the mixture stirred for 30 min. All volatiles were removed under reduced pressure at –80 °C and then for 5 min at –40 °C. *Ortho*-difluorobenzene (3-4 ml) was condensed on top at –35 °C and the mixture stirred for 5 min at around –35 °C until a grey precipitate was formed. The yellowish solution was decanted off. The precipitate was cooled to –80 °C and dichloromethane (3-4 ml) condensed on top, stirred for 1 min until everything was dissolved and filtered at –80 °C. All volatiles were removed from the filtrate under reduced pressure at –35 °C, and the residue was washed two times with *ortho*-difluorobenzene. The residual solvent was removed under reduced pressure and pure **1** was obtained as colourless powder (yield: 28 %).

^{1}H NMR (401 MHz, CD_2Cl_2, 20 °C): δ=7.05 (s, 4H-Ar), 4.31 (s, 4H, NCH_2CH_2N), 2.32 (s, 18H, CH_3) ppm.[14]

^{19}F NMR (377 MHz, CD_2Cl_2, 20 °C): δ=–216.8 (t, 1F, trans-F, $^2J(^{19}F,^{19}F)$=49 Hz), –315.7 (d, 2F, cis-F) ppm.[14]

^{13}C NMR (101 MHz, CD_2Cl_2, 20 °C): δ=152.4 (NCN carbene), 140.9 (C aromatic), 136.5 (C aromatic), 131.0 (C aromatic), 130.0 (C aromatic), 51.4 (CH_2 imidazolidine), 20.8 (CH_3), 17.2 (CH_3) ppm.[14]

IR (ATR, 25 °C): $\tilde{\nu}$=424 (m), 480 (w), 528 (s, $\nu(\mathrm{AuF_{terminal}})$), 574 (s, $\nu_s(\mathrm{AuF_2})$), 604 (s, $\nu_s(\mathrm{AuF_2})$), 648 (w), 738 (w), 761 (w), 853 (m), 932 (w), 956 (w), 982 (w), 1015 (m), 1034 (m), 1101 (w), 1170 (w), 1179 (w), 1190 (w), 1221 (w), 1273 (s), 1326 (m), 1381 (m), 1465 (m), 1483 (m), 1506 (m), 1543 (s), 1607 (m), 1630 (w), 2874 (w), 2921 (m), 2968 cm^{-1} (w).

FT-Raman (25 °C): $\tilde{\nu}$=140 (m), 242 (m), 260 (w), 282 (w), 295 (m, $\nu(\mathrm{AuC})$), 340 (w), 427 (w), 474 (w), 503 (w), 531 (m, $\nu(\mathrm{AuF_{terminal}})$), 574 (s, $\nu_s(\mathrm{AuF_2})$), 764 (w), 804 (w), 958 (w), 1021 (w), 1314 (m), 1385 (m), 1454 (w), 1470 (m), 1510 (m), 1607 (m), 2865 (m), 2922 (s), 2952 cm^{-1} (w).

Comment on the Synthesis and Purification of [AuF_3(SIMes)], 1

The recent report on the synthesis of [AuF_3(SIMes)] (**1**) from the precursors AuF_3 and the free carbene SIMes does not yield compound **1** quantitatively but the isolated sample contains minor products that strongly depend on the reaction conditions.[14] One of the main side products of the reaction in dichloromethane was identified as [$Au(SIMes)_2$][AuF_4] by NMR spectroscopy. Its formation can be explained by reaction of **1** with unreacted AuF_3 to form [$Au(SIMes)_2$][AuF_4]. Cationic [AuF_2(SIMes)]$^+$ most certainly is not stable under these conditions and likely decomposes very quick e.g. by fluorination of the solvent and subsequent reductive elimination to an Au^I species that seems to be stable enough to react with a second SIMes molecule (Scheme S-1). The side product [$Au(SIMes)_2$][AuF_4] can be extracted at –35 °C in *ortho*-difluorobenzene and compound **1** remains as pure product (see experimental section).

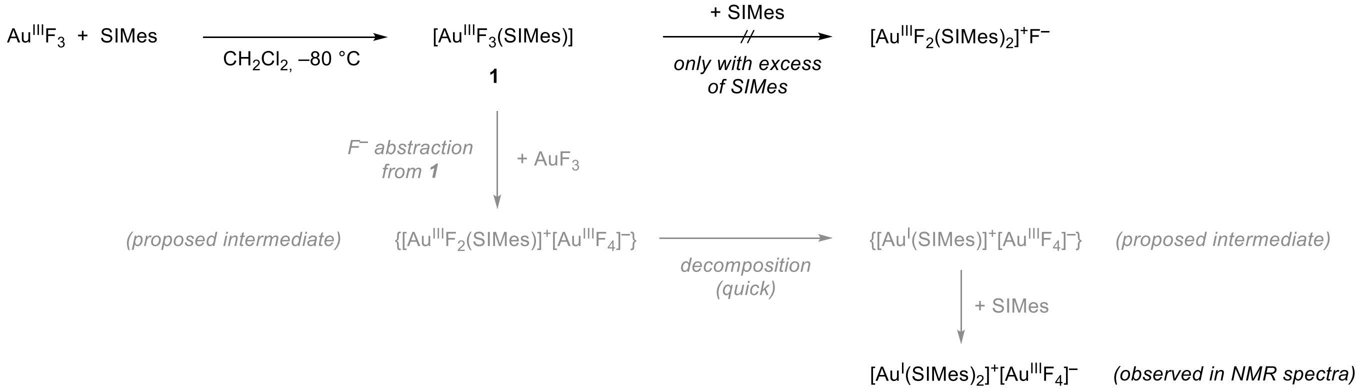

Scheme S-1. Proposed mechanism for the formation of the side product [$Au(SIMes)_2$][AuF_4] in the reaction of AuF_3 with SIMes in CH_2Cl_2 at –80 °C. Experimentally observed species (black) are differentiated from proposed intermediates (grey).

Synthesis of [AuClF$_2$(SIMes)], 2

To a sample of compound **1** (3.5 mg, 6 µmol) dichloromethane (1-2 ml) and Me$_3$SiCl (15 mg, 140 µmol, 23 eq) were condensed at –196 °C. The mixture was warmed to –30 °C, stirred for 5 min and all volatiles were removed under reduced pressure. Compound **2** was obtained as pure substance.

^{1}H NMR (401 MHz, CD$_2$Cl$_2$, 20 °C): δ=7.05 (s, 4H-Ar), 4.28 (s, 4H, NCH$_2$CH$_2$N), 2.34 (s, 18H, CH$_3$) ppm.

^{19}F NMR (377 MHz, CD$_2$Cl$_2$, 20 °C): δ=–325.9 (s, 2F, Au-F) ppm.

^{13}C NMR (101 MHz, CD$_2$Cl$_2$, 20 °C): δ=166.0 (NCN carbene), 140.7 (C aromatic), 136.5 (C aromatic), 131.5 (C aromatic), 130.0 (C aromatic), 51.5 (CH$_2$ imidazolidine), 20.9 (CH$_3$), 17.2 (CH$_3$) ppm.

IR (ATR, 25 °C): $\tilde{\nu}$=423 (w), 498 (w), 566 (m, ν_s(AuF$_2$)), 576 (m), 594 (vs, ν_{as}(AuF$_2$)), 637 (m), 713 (m), 738 (m), 820 (w), 854 (s), 925 (w), 951 (m), 986 (m), 1018 (m), 1030 (m), 1168 (w), 1186 (m), 1222 (m), 1276 (s), 1319 (m), 1377 (m), 1459 (m), 1479 (m), 1540 (s), 1607 (m), 1734 (w), 2866 (w), 2924 (w), 2968 (m), 3021 cm^{-1} (w).

FT-Raman (25 °C): $\tilde{\nu}$=126 (m), 170 (w), 187 (m), 234 (w), 254 (w), 286 (m, ν(AuC)), 339 (m, ν(AuCl)), 364 (w), 420 (w), 474 (w), 500 (w), 567 (s, ν_s(AuF$_2$)), 578 (m), 953 (w), 988 (w), 1019 (w), 1170 (w), 1221 (w), 1315 (m), 1382 (m), 1462 (m), 1508 (m), 1607 (m), 2737 (w), 2860 (w), 2924 (s), 2960 (m), 3005 (m), 3017 cm^{-1} (m).

Crystal growth of [AuClF$_2$(SIMes)], 2

Crystals of [AuClF$_2$(SIMes)] were grown from a solution of [AuClF$_2$(SIMes)] in CH$_2$Cl$_2$ (ca. 3 mg in 1 ml). In the side arm of a Y-shaped glass tube with Teflon sealing n-pentane (ca. 2 ml) was added and the reactor stored for 1 week at 5 °C. Small crystals of [AuClF$_2$(SIMes)] were obtained.

Synthesis of [AuF$_2$(OTeF$_5$)(SIMes)], 3

To a pure sample of compound **1** (3.5 mg, 6 µmol) dichloromethane (1-2 ml) and Me$_3$Si(OTeF$_5$) (44 mg, 140 µmol, 23 eq) were condensed at –196 °C. The mixture was warmed to –30 °C, stirred for 5 min and all volatiles were removed under reduced pressure. Compound **4** was obtained as pure substance.

^{1}H NMR (401 MHz, CD$_2$Cl$_2$, 20 °C): δ=7.07 (s, 4H-Ar), 4.37 (s, 4H, NCH$_2$CH$_2$N), 2.34 (s, 18H, CH$_3$) ppm.

^{19}F NMR (377 MHz, CD$_2$Cl$_2$, 20 °C): δ=–34.6 (X$_4$**Y**, 1F, OTeF axial, $^2J(^{19}F_X,^{19}F_Y)$=182 Hz), –41.8 (**X$_4$**Y, 4F, OTeF$_4$ equatorial, $^1J(^{19}F_X,^{125}Te)$=3160 Hz, $^4J(^{19}F_X,^{19}F_A)$=1.7 Hz), –310.5 (d, 2F, Au-F$_A$) ppm.

^{13}C NMR (101 MHz, CD$_2$Cl$_2$, 20 °C): δ=149.4 (NCN carbene), 141.1 (C aromatic), 136.3 (C aromatic), 131.6 (C aromatic), 130.0 (C aromatic), 51.5 (CH$_2$ imidazolidine), 20.9 (CH$_3$), 17.2 (CH$_3$) ppm.

IR (ATR, 25 °C): $\tilde{\nu}$=424 (m), 446 (w), 472 (m), 490 (s), 557 (m), 569 (m), 573 (m, ν_s(AuF$_2$)), 593 (w), 613 (s, ν_s(AuF$_2$)), 645 (m), 675 (vs), 689 (s), 712 (s), 737 (w), 761 (m), 812 (s, ν(AuOTe)), 854 (m), 908 (w), 955 (w), 972 (w), 980 (w), 1013 (m), 1029 (w), 1034 (w), 1155 (w), 1170 (w), 1190 (w), 1218 (m), 1282 (s), 1323 (m), 1382 (m), 1464 (m), 1481 (m), 1507 (m), 1557 (s), 1608 (m), 1632 (w), 2869 (w), 2926 (m), 2964 (m), 2975 cm^{-1} (m).

Crystal growth of [$AuF_2(OTeF_5)$(SIMes)], 3

Crystals of [$AuF_2(OTeF_5)$(SIMes)]·CH_2Cl_2 (**3a**) were grown from a solution of [$AuF_2(OTeF_5)$(SIMes)] in CH_2Cl_2 (ca. 3 mg in 1 ml). In the side arm of a Y-shaped glass tube with Teflon sealing n-pentane (ca. 2 ml) was added and the reactor stored for 1 week at 5 °C. Small crystals of [$AuF_2(OTeF_5)$(SIMes)]·CH_2Cl_2 that were obtained.

Crystals of [$AuF_2(OTeF_5)$(SIMes)]·0.4($C_6F_2H_4$)·0.4($HOTeF_5$) (**3b**) were grown from a solution of [$AuF_2(OTeF_5)$(SIMes)] in *ortho*-difluorobenzene (ca. 3 mg in 1 ml). In the side arm of a Y-shaped glass tube with Teflon sealing n-pentane (ca. 2 ml) was added and the reactor stored for 1 week at 5 °C. Small and middle sized crystals of [$AuF_2(OTeF_5)$(SIMes)]·0.4($C_6F_2H_4$)·0.4($HOTeF_5$) were obtained.

Synthesis of $Me_3Si(OTeF_5)$

At –196 °C $HOTeF_5$ (5.6 g, 24 mmol) was condensed into a flask, warmed to –78 °C and Me_3SiCl (2.6 g, 24 mmol, 1 eq) added with a syringe under argon flow. The mixture was warmed to –30 °C, stirred for 1 h and purified by removal of HCl under reduced pressure at –50 °C until no more HCl was visible in the IR spectrum of the gas phase. Compound **3** was obtained as colourless liquid (m.p. –52 °C).

^1H NMR (401 MHz, CD_2Cl_2, 20 °C): δ=0.37 (m, 9H, CH_3) ppm.

^{19}F NMR (377 MHz, CD_2Cl_2, 20 °C): δ=–39.1 (X_4**Y**, 1F, OTeF axial, $^1J(^{19}F_Y,^{125}Te)$=3425 Hz, $^2J(^{19}F_X,^{19}F_Y)$=187 Hz), –42.3 (**X_4**Y, 4F, $OTeF_4$ equatorial, $^1J(^{19}F_X,^{125}Te)$=3576 Hz) ppm.

^{13}C NMR (101 MHz, CD_2Cl_2, 20 °C): δ=0.8 (CH_3) ppm.

$^{29}Si\{^1H\}$ NMR (77 MHz, neat, ext. acetone-[d_6], 20 °C): δ=37.2 (p, $^3J(^{19}F_X,^{29}Si)$=1.5 Hz, $^2J(^{29}Si,^{125}Te)$=112 Hz, $^2J(^{29}Si,^{123}Te)$=60 Hz) ppm.

IR (gas cuvette with Si windows, ca. 20 mbar, 25 °C): $\tilde{\nu}$=506 (w), 639 (w), 723 (s), 764 (m), 858 (s), 931 (s, ν_{as}(SiOTe)), 1014 (w), 1267 (m), 1431 (w), 2914 (w), 2973 cm^{-1} (w).

FT-Raman (25 °C): $\tilde{\nu}$=168 (m), 175 (m), 194 (m), 215 (m), 224 (m), 251 (m), 295 (w), 301 (m, δ(TeF_5)), 331 (m, δ(SiOTe)), 341 (w), 506 (s, ν_s(SiOTe)), 644 (s), 693 (s), 779 (m), 906 (m), 1260 (w), 1422 (m), 2912 (s), 2974 cm^{-1} (s).

Crystal growth of $Me_3Si(OTeF_5)$

Crystals of $Me_3Si(OTeF_5)$ were grown from $Me_3Si(OTeF_5)$ as neat substance by its slow evaporation at –50 °C and desublimation at –78 °C under static vacuum (approximately 10^{-2} mbar) in a glass apparatus over a period of about 3 h. Middle sized crystals of $Me_3Si(OTeF_5)$ were obtained, that were suitable for single crystal X-ray diffraction.

X-ray crystallography

Table S-1. Crystal data and refinement details for the crystal structure analysis of [$AuClF_2$(SIMes)], [$AuF_2(OTeF_5)$(SIMes)]·X and $Me_3Si(OTeF_5)$.

	[$AuClF_2$(SIMes)], 2	**[$AuF_2(OTeF_5)$(SIMes)], 3a** ·CH_2Cl_2	**[$AuF_2(OTeF_5)$(SIMes)], 3b** ·0.4($C_6F_2H_4$)·0.4($HOTeF_5$)	$Me_3Si(OTeF_5)$
empirical formula	$C_{21}H_{26}AuClF_2N_2$	$C_{21}H_{26}AuF_7N_2OTe$, CH_2Cl_2	$C_{21}H_{26}AuF_7N_2OTe$, 0.4($C_6H_5F_7OTe$)	$C_3H_9F_5OSiTe$
formula weight	576.85	864.93	912.26	311.79
crystal system	orthorhombic	triclinic	monoclinic	monoclinic
space group	*Pnma*	$P\bar{1}$	*C2/c*	$P2_1/c$
a / Å	14.7369(9)	9.5656(5)	45.692(3)	6.2372(6)
b / Å	20.2843(14)	9.8860(4)	10.1726(6)	19.3447(18)
c / Å	7.0652(5)	16.5307(8)	33.134(2)	8.1649(8)
α / °	-	94.667(2)	-	-
β / °	-	95.131(2)	130.894(2)	108.024(5)
γ / °	-	116.737(2)	-	-
volume / Å^3	2112.0(2)	1377.45(12)	11641.8(12)	936.81(16)
Z	4	2	16	4
ρ_{calc} / g·cm^{-3}	1.814	2.085	2.082	2.211
μ / mm^{-1}	7.117	6.638	6.488	3.331
F(000)	1120	820	6866	584
crystal size / mm^3	0.24 × 0.15 × 0.11	0.28 x 0.28 x 0.09	0.27 x 0.10 x 0.08	0.52 x 0.26 x 0.18
temperature during collection / K	110	100	100	100
2θ range for data collection / °	2.764 – 30.544	2.329 – 30.571	2.359 – 30.601	2.827 – 26.416
reflection collected	32517	28287	271977	9146
independent reflections	3304	8460	17899	1917
R_{int}	0.0445	0.0319	0.0470	0.0303
data / restraints / parameters	3304 / 0 / 177	8460 / 0 / 331	17899 / 0 / 742	1917 / 0 / 136
[a] goodness-of-fit on F^2	1.118	1.065	1.159	1.152
[b,c] final *R* indexes [I≥2σ (I)], R_1 / ωR_2	0.0203 / 0.0435	0.0306 / 0.0556	0.0533 / 0.1434	0.0203 / 0.0412
final *R* indexes [all data]	0.0234 / 0.0444	0.0401 / 0.0581	0.0598 / 0.1488	0.0259 / 0.0415
largest diff. [peak / hole / e·Å^{-3}]	0.577 / –1.529	2.802 / –1.610	5.387 / –2.153	0.337 / –0.555
CCDC reference[d]	1850339	1849407	1850338	1851138

[a] $S = \{\sum[w(F_o^2-F_c^2)^2]/(n-p)\}^{0.5}$; n = no. of reflections; p = no. of parameters. [b] $R_1 = \sum||F_0|-|F_c||/\sum|F_0|$. [c] $wR_2 = \{\sum[w(F_o^2-F_c^2)^2]/\sum[w(F_o^2)^2]\}^{0.5}$. [d] data are available free of charge via “*www.ccdc.cam.ac.uk/data_request/cif*”.

Structure of [AuClF$_2$(SIMes)], 2

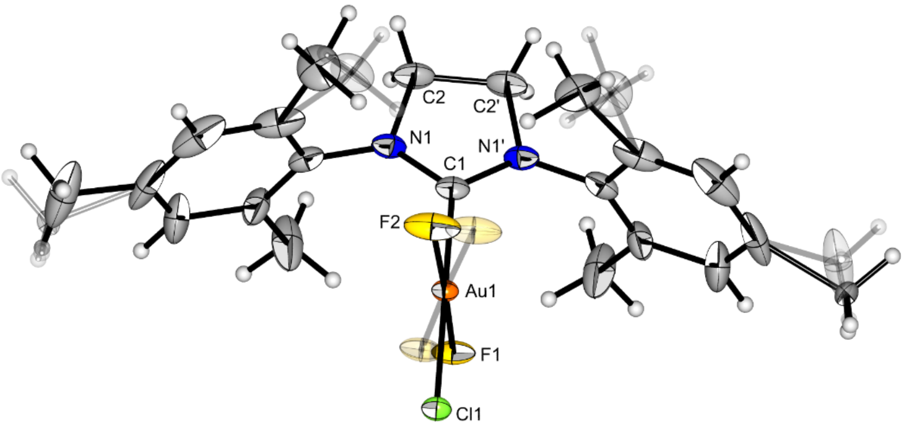

Figure S-1. Molecular structure of [AuClF$_2$(SIMes)] (**2**) in the solid state. Bond lengths to the Au$^{\mathrm{III}}$ centre are F1-Au 192.0(2) pm, F2-Au 193.1(2) pm, Cl1-Au 230.2(1) pm, C1-Au 200.8(3) pm. Thermal ellipsoids are set at 50% probability. The second position of disordered atoms are shown as transparent ellipsoids.

Structure of [AuF$_2$(OTeF$_5$)(SIMes)]·CH$_2$Cl$_2$, 3a

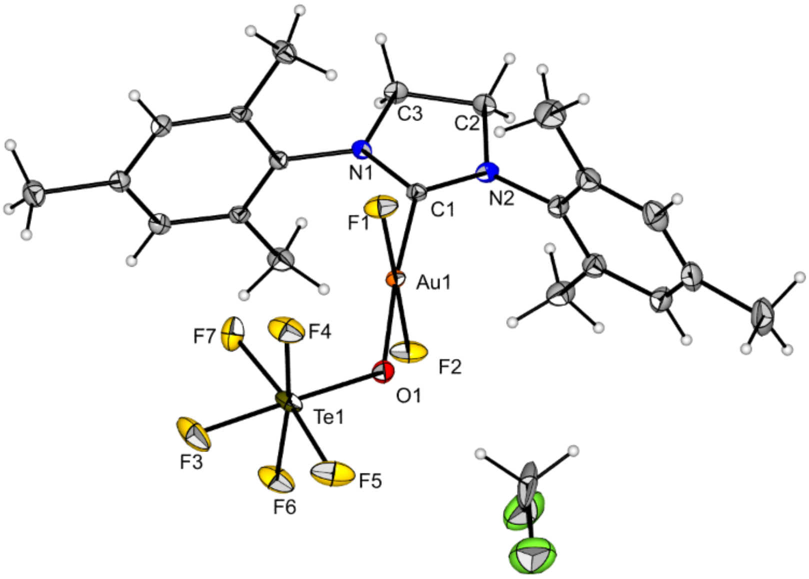

Figure S-2. Molecular structure of [AuF$_2$(OTeF$_5$)(SIMes)]·CH$_2$Cl$_2$ (**3a**) in the solid state with the CH$_2$Cl$_2$ molecule. Bond lengths to the Au$^{\mathrm{III}}$ centre are F1-Au 191.5(2) pm, F2-Au 192.0(2) pm, O1-Au 205.7(4) pm, C1-Au 196.9(5) pm. The closest C–(H)–F distance is between F2 and the CH$_2$Cl$_2$ molecule and is 321.7(6) pm long. The closest C–(H)–O distance is 358.7(6) pm and between O1 and the CH$_2$Cl$_2$ molecule. Thermal ellipsoids are set at 50% probability.

Structure of $[AuF_2(OTeF_5)(SIMes)]\cdot0.4(C_6F_2H_4)\cdot0.4(HOTeF_5)$, 3b

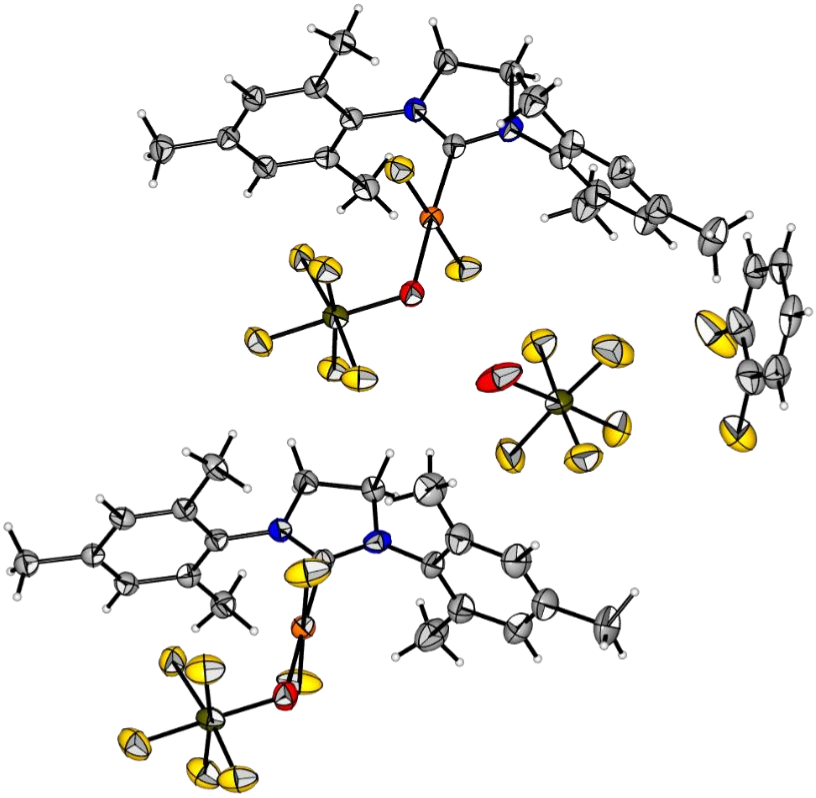

Figure S-3. Molecular structure of $[AuF_2(OTeF_5)(SIMes)]\cdot0.4(C_6F_2H_4)\cdot0.4(HOTeF_5)$ (**3b**) in the solid state. The asymmetric unit contains two $[AuF_2(OTeF_5)(SIMes)]$ units and the $HOTeF_5$ and $C_6H_4F_2$ molecules with a chemical occupancy of 0.667. There is a possible O–(H)–O contact (334.4(10) pm) between the OH group of the $HOTeF_5$ molecule and the oxygen atom of one $[AuF_2(OTeF_5)(SIMes)]$ molecule. Thermal ellipsoids are set at 50% probability.

NMR spectroscopy

Summary of NMR parameters

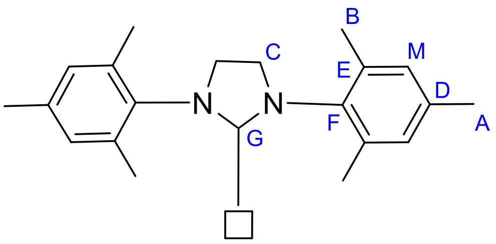

Scheme S-2. Structure and assignment of complexes containing the SIMes ligand [AuF_3(SIMes)] (**1**), [$AuClF_2$(SIMes)] (**2**) and [$AuF_2(OTeF_5)$(SIMes)] (**3**).

Table S-2. Summary of ^{1}H, ^{19}F and ^{13}C chemical shifts and coupling constants for the compounds [AuF_3(SIMes)] (**1**), [$AuClF_2$(SIMes)] (**2**) and [$AuF_2(OTeF_5)$(SIMes)] (**3**). All NMR chemical shifts are given in ppm and coupling constants in Hz. The compounds were measured in CD_2Cl_2 at 20 °C. The ^{19}F NMR chemical shifts and coupling constants of [$AuF_2(OTeF_5)$(SIMes)] were simulated for determination (see Figure S-6).

	[AuF_3(SIMes)], 1 [a]	**[$AuClF_2$(SIMes)], 2**	**[$AuF_2(OTeF_5)$(SIMes)], 3**
δ F_{cis} (2F)	–315.7 (d)	–325.9 (s)	–310.5 (p)
δ F_{trans} (1F)	–216.8 (t)	--	--
δ F_Y (1F)	--	--	–34.6
δ F_X (4F)	--	--	–41.8
δ H_M (4H)	7.05 (m)	7.05 (m)	7.07 (m)
δ H_C (4H)	4.31 (s)	4.28 (s)	4.37 (s)
δ H_B (12H)	2.32 (s)	2.34 (s)	2.34 (s)
δ H_A (6H)	2.32 (s)	2.34 (s)	2.34 (s)
δ C_G	152.4	166.0	149.4
δ $C_{aromatic}$	130.0, 136.5, 131.0, 140.9	130.0, 136.5, 131.5, 140.7	130.0, 136.3, 131.6, 141.1
δ C_C	51.4	51.5	51.5
δ C_B	17.2	17.2	17.2
δ C_A	20.8	20.9	20.9
	$^{2}J(^{19}F_{cis},^{19}F_{trans}) = 49$	--	$^{2}J(^{19}F_X,^{19}F_Y) = 182$ $^{4}J(^{19}F_X,^{19}F_{cis}) = 1.7$ $^{4}J(^{19}F_Y,^{19}F_{cis}) = 0.3$ $^{1}J(^{19}F_X,^{125}Te) = 3160$

[a] values have been reported before[14]

Spectra of [AuF$_3$(SIMes)], 1

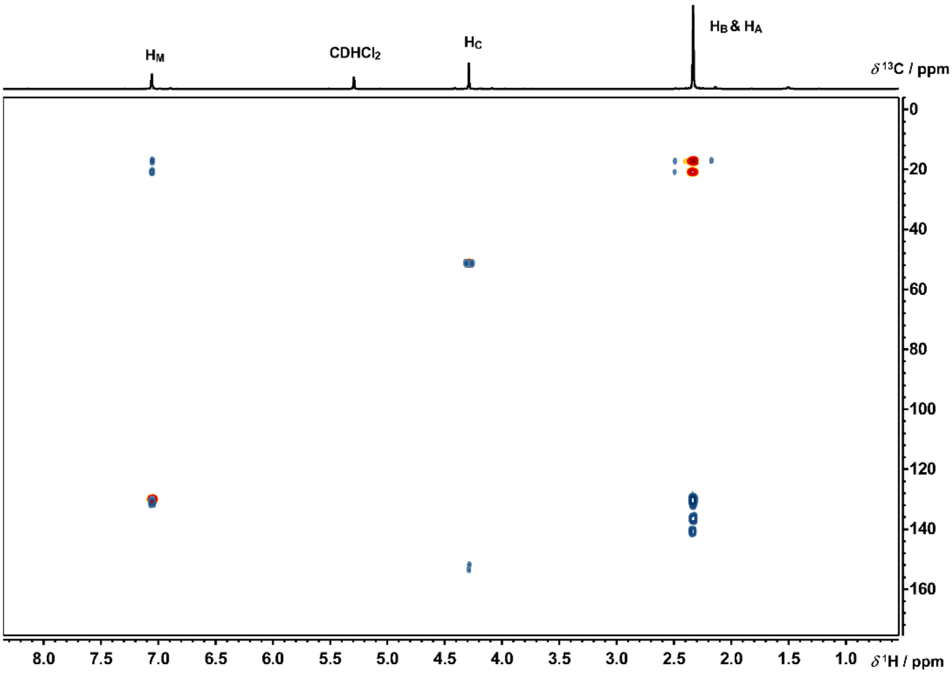

Figure S-4. ^{1}H,^{13}C HMBC NMR spectrum (blue, foreground, optimized on a coupling constant of 8 Hz) and ^{1}H,^{13}C HMQC (red, background, optimized on a coupling constant of 140 Hz) of pure [AuF$_3$(SIMes)] in CD$_2$Cl$_2$ (20 °C, 401 & 101 MHz). The ^{1}H NMR spectrum is also shown including the assignment (top). Characteristic is the crosspeak of H$_C$ to the carbene carbon C$_G$ at 152.4 ppm on the ^{13}C NMR chemical shift scale that corresponds to the $^{3}J(^{1}H_C,^{13}C_G)$ coupling.

Spectra of [AuClF$_2$(SIMes)], 2

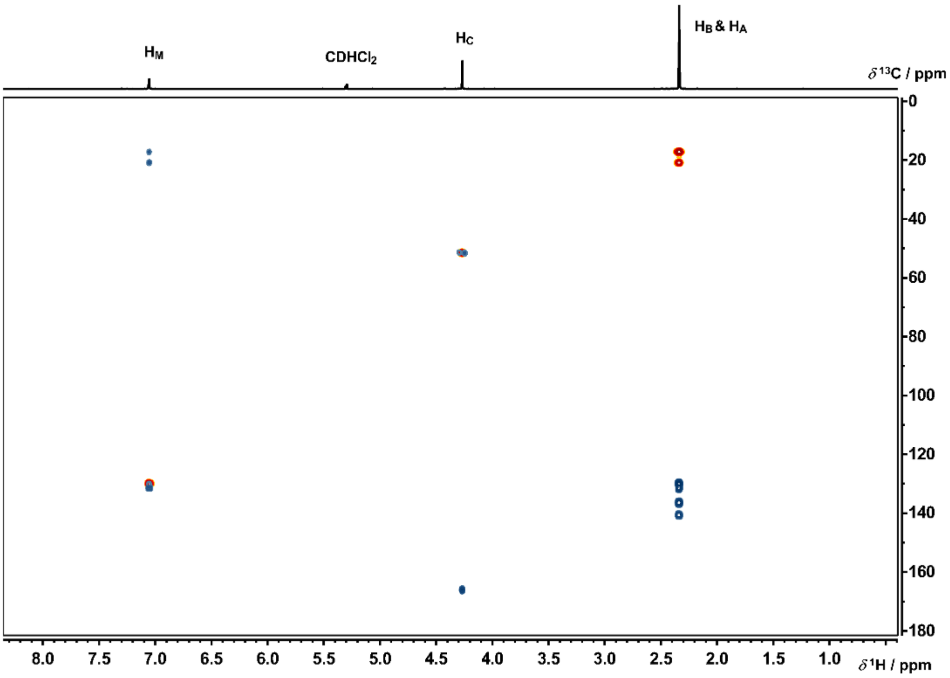

Figure S-5. ^{1}H,^{13}C HMBC NMR spectrum (blue, foreground, optimized on a coupling constant of 8 Hz) and ^{1}H,^{13}C HMQC (red, background, optimized on a coupling constant of 140 Hz) of pure [AuClF$_2$(SIMes)] in CD$_2$Cl$_2$ (20 °C, 401 & 101 MHz). The ^{1}H NMR spectrum is also shown including the assignment (top). Characteristic is the crosspeak of H$_C$ to the carbene carbon C$_G$ at 166.0 ppm on the ^{13}C NMR chemical shift scale that corresponds to the $^{3}J(^{1}H_C,^{13}C_G)$ coupling.

Spectra of [$AuF_2(OTeF_5)(SIMes)$], 3

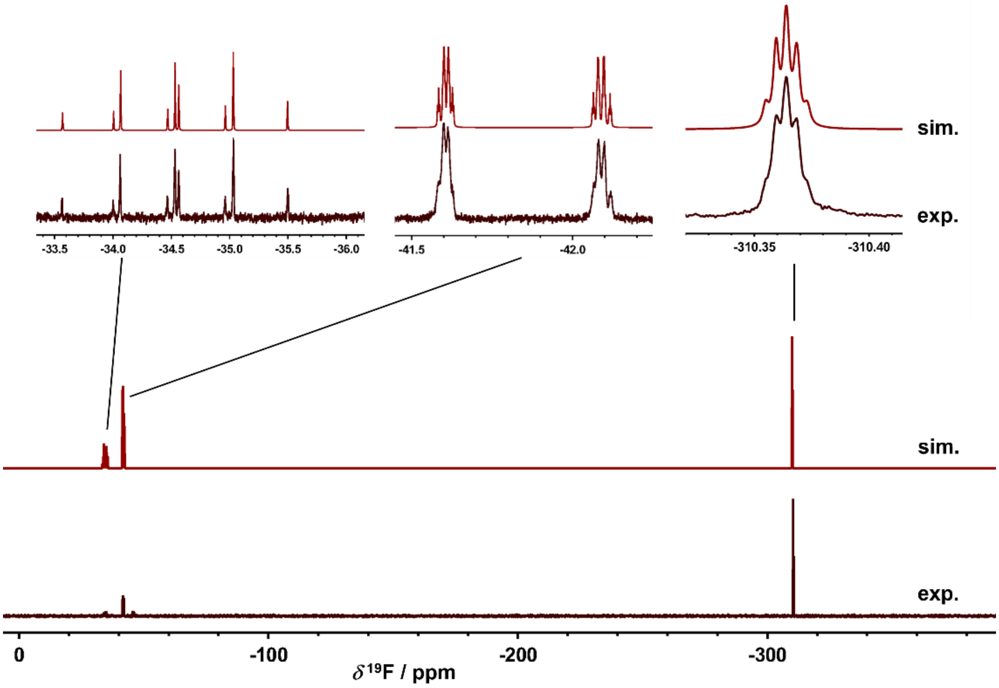

Figure S-6. ^{19}F NMR spectrum of [$AuF_2(OTeF_5)(SIMes)$] in CD_2Cl_2 (20 °C, 376 MHz). Shown are both, the experimental (bottom) and the simulated spectrum (top) as well as enlarged sections of the resonances. The NMR parameters from the simulation are summarised in Table S-2.

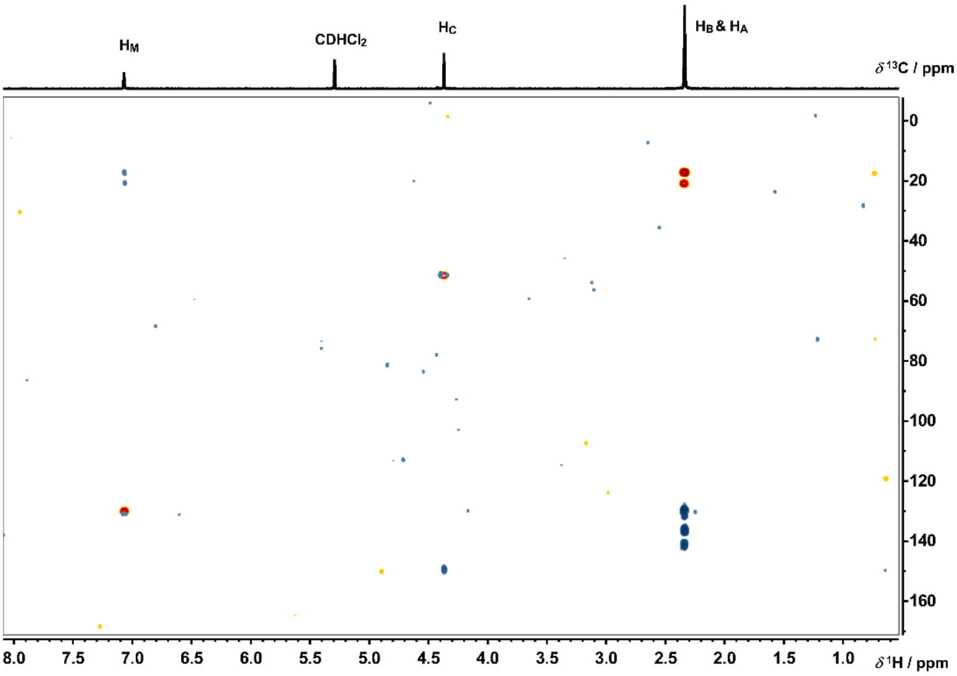

Figure S-7. $^{1}H,^{13}C$ HMBC NMR spectrum (blue, foreground, optimized on a coupling constant of 8 Hz) and $^{1}H,^{13}C$ HMQC (red, background, optimized on a coupling constant of 140 Hz) of pure [$AuF_2(OTeF_5)(SIMes)$] in CD_2Cl_2 (20 °C, 401 & 101 MHz). The ^{1}H NMR spectrum is also shown including the assignment (top). Characteristic is the crosspeak of H_C to the carbene carbon C_G at 149.4 ppm on the ^{13}C NMR chemical shift scale that corresponds to the $^{3}J(^{1}H_C,^{13}C_G)$ coupling.

Vibrational spectroscopy

Overview

Table S-3. Stretching modes of the ligands bound to the gold(III) centre of [AuF_3(SIMes)], [$AuClF_2$(SIMes)] and [$AuF_2(OTeF_5)$(SIMes)] plus comparison of IR and Raman frequencies with the calculated values (RI-B3LYP-D3/def2-TZVPP).

	[AuF_3(SIMes)], 1			**[$AuClF_2$(SIMes)], 2**			**[$AuF_2(OTeF_5)$(SIMes)], 3**		
	IR	Raman	*calc.*	IR	Raman	*calc.*	IR	Raman	*calc.*
ν_s(AuC)	[c]	295	*291*	[c]	286	*280*	[c]	[b]	*294*
ν($AuCl_{term}$)	--	--	--	[c]	339	*346*	--	--	--
ν_s(AuF_2)	574	574	*554*	566	567	*553*	573	[b]	*564*
ν_{as}(AuF_2)	604	[a]	*588*	594	[a]	*582*	613	[a, b]	*598*
ν(AuF_{term})	528	531	*577*	--	--	--	--	--	--
ν(AuOTe)	--	--	--	--	--	--	812	[b]	*784*

[a] band not Raman active. [b] sample was destroyed during Raman measurement. No spectrum available. [c] IR spectra were only recorded in the range of 400 – 4000 cm^{-1} (no far-IR available).

Spectra of [AuF_3(SIMes)], 1

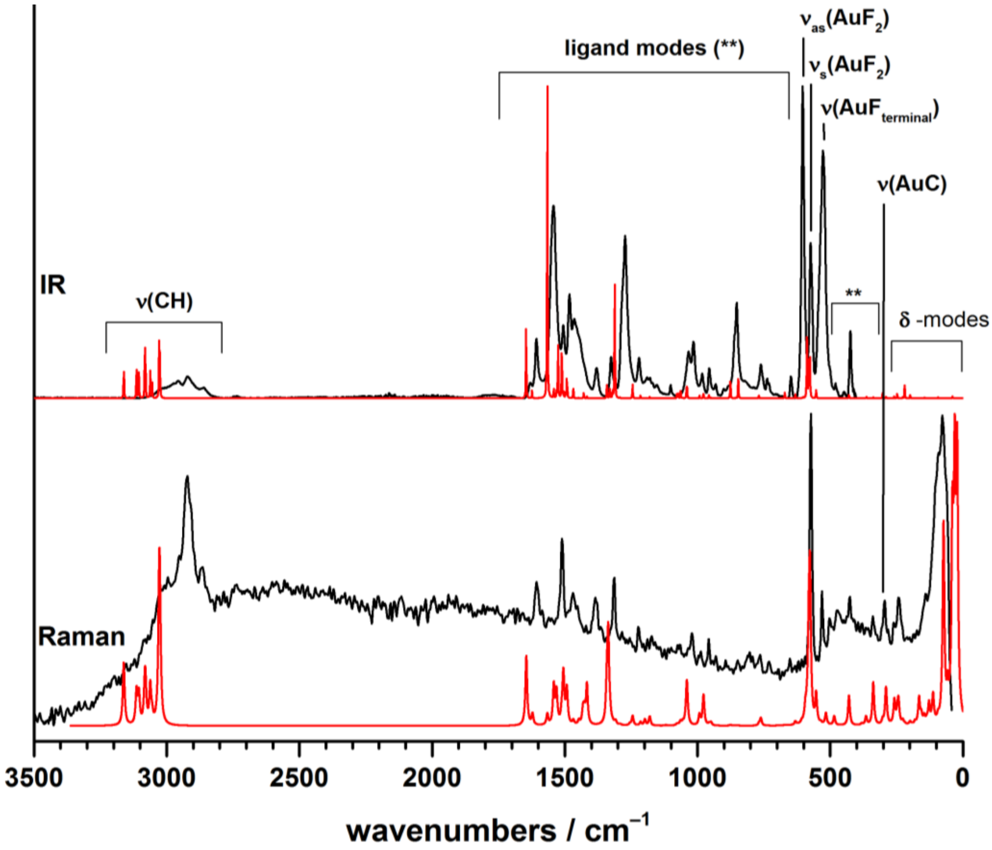

Figure S-8. Comparison of experimental (black line, broad bands) and calculated (red line, sharp bands, RI-B3LYP-D3/def2-TZVPP) IR (top) and Raman spectrum (bottom) of [AuF_3(SIMes)]. In the experimental Raman spectrum also a strong gold fluorescence is visible as very broad underground. The stretching modes of all ligands bound to the gold centre are assigned. Modes that belong to the SIMes ligand were not assigned in detail. Exact values are given in Table S-3 and in the experimental section.

Spectra of $[AuClF_2(SIMes)]$, 2

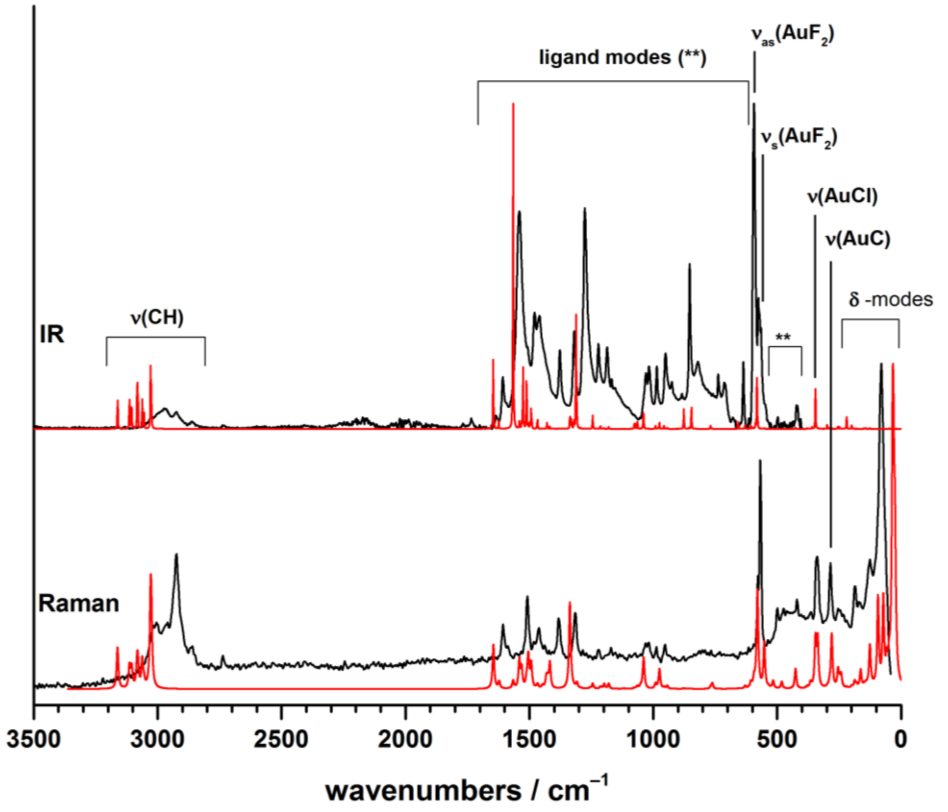

Figure S-9. Comparison of experimental (black line, broad bands) and calculated (red line, sharp bands, RI-B3LYP-D3/def2-TZVPP) IR (top) and Raman spectrum (bottom) of $[AuClF_2(SIMes)]$. The stretching modes of all ligands bound to the gold centre are assigned. Modes that belong to the SIMes ligand were not assigned in detail. Exact values are given in Table S-3 and in the experimental section.

Spectra of $[AuF_2(OTeF_5)(SIMes)]$, 3

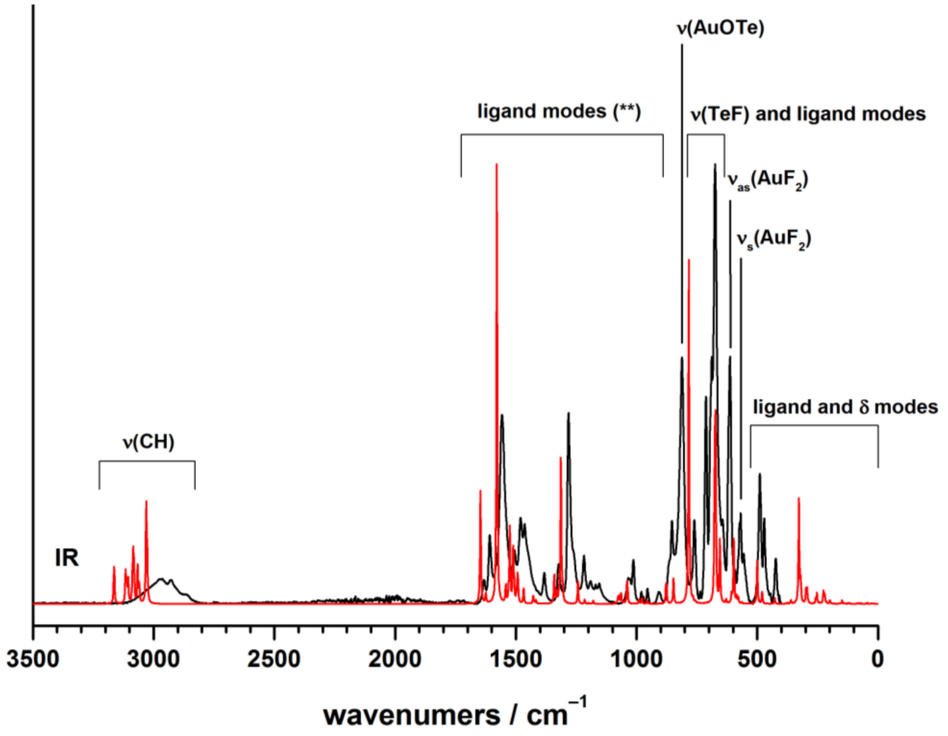

Figure S-10. Comparison of experimental (black line, broad bands) and calculated (red line, sharp bands, RI-B3LYP-D3/def2-TZVPP) IR spectrum of $[AuF_2(OTeF_5)(SIMes)]$. The stretching modes of all ligands bound to the gold centre are assigned. Modes that belong to the SIMes ligand were not assigned in detail. Exact values are given in Table S-3 and in the experimental section.

Spectra of $Me_3Si(OTeF_5)$

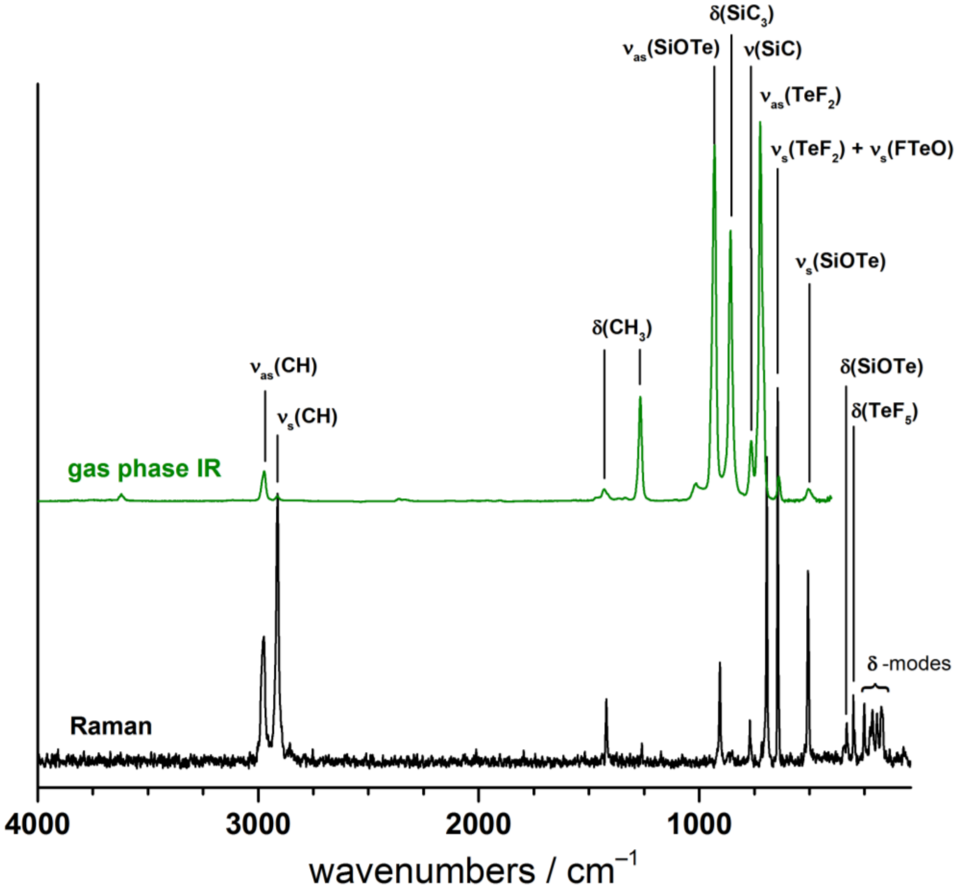

Figure S-11. IR (top, green) and Raman spectrum (bottom, black) of $Me_3Si(OTeF_5)$. Bands were assigned with the aid of quantum chemical calculation on the RI-B3LYP-D3/def2-TZVPP level of theory. Exact values are given in the experimental section.

Quantum-chemical calculations

Comparison of SIMes affinity with FIA values

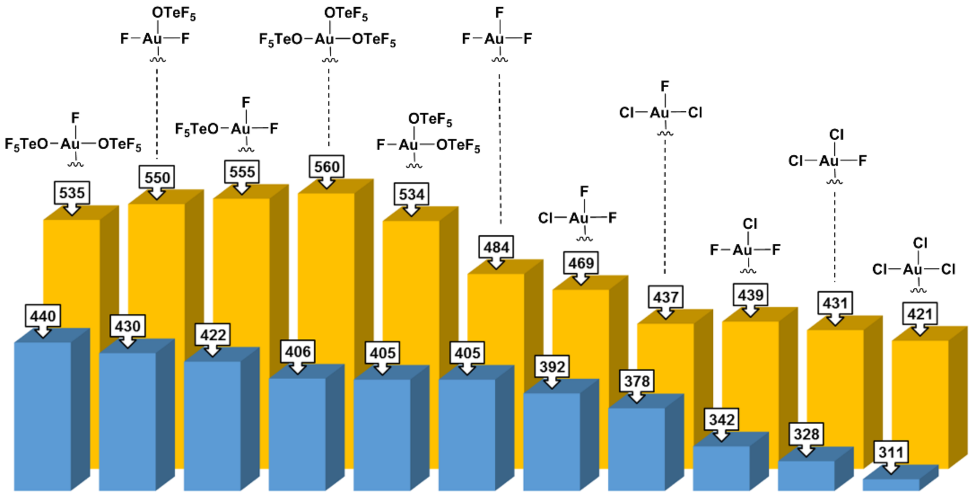

Figure S-12. Comparison of the calculated SIMes affinity (front, blue) on the RI-B3LYP-D3/def2-TZVPP level of theory with the fluoride ion affinities (FIA, back, orange) on RI-BP86/def-SV(P) level of theory according to Krossing et al.[15,16] All values are given in $kJ\cdot mol^{-1}$ and are in case of SIMes affinity free reaction enthalpies at 273K and in case of FIA the change in the SCF energies corrected by the zero point energies.

References

1 A. G. Sharpe, *J. Chem. Soc.*, 1949, 2901.

2 M. A. Ellwanger, S. Steinhauer, P. Golz, H. Beckers, A. Wiesner, B. Braun-Cula, T. Braun and S. Riedel, *Chem. Eur. J.*, 2017, **23**(54), 13501.

3 K. Seppelt and D. Nothe, *Inorg. Chem.*, 1973, **12**(11), 2727.

4 A. J. Arduengo, III, J. R. Goerlich and W. J. Marshall, *J. Am. Chem. Soc.*, 1995, **117**(44), 11027.

5 G. M. Sheldrick, *Acta Crystallogr. A*, 2008, **64**, 112.

6 G. M. Sheldrick, *Acta Crystallogr. C*, 2015, **71**, 3.

7 O. V. Dolomanov, L. J. Bourhis, R. J. Gildea, J. A. K. Howard and H. Puschmann, *J. Appl. Crystallogr.*, 2009, **42**(2), 339.

8 A. D. Becke, *J. Chem. Phys.*, 1993, **98**(7), 5648.

9 M. Sierka, A. Hogekamp and R. Ahlrichs, *J. Chem. Phys.*, 2003, **118**(20), 9136.

10 S. Grimme, J. Antony, S. Ehrlich and H. Krieg, *J. Chem. Phys.*, 2010, **132**(15), 154104.

11 F. Weigend, M. Häser, H. Patzelt and R. Ahlrichs, *Chem. Phys. Lett.*, 1998, **294**(1-3), 143.

12 F. Weigend and R. Ahlrichs, *Phys. Chem. Chem. Phys.*, 2005, **7**(18), 3297.

13 TURBOMOLE GmbH, *TURBOMOLE V7.0.1*, a development of University of Karlsruhe and Forschungszentrum Karlsruhe GmbH, 1989–2015.

14 M. A. Ellwanger, S. Steinhauer, P. Golz, T. Braun and S. Riedel, *Angew. Chem. Int. Ed.*, 2018, **57**(24), 7210 (*Angew. Chem.*, 2018, **130**(24), 7328).

15 K. O. Christe, D. A. Dixon, D. McLemore, W. W. Wilson, J. A. Sheehy and J. A. Boatz, *J. Fluorine Chem.*, 2000, **101**(2), 151.

16 H. Böhrer, N. Trapp, D. Himmel, M. Schleep and I. Krossing, *Dalton Trans.*, 2015, **44**(16), 7489.